

# Real-time visualization of neural synchrony for identifying coordinated cell assemblies

Jason M. Samonds<sup>a</sup>, A.B. Bonds<sup>a,b,\*</sup>

<sup>a</sup> Department of Biomedical Engineering, Vanderbilt University, 5824 Stevenson Center, Nashville, TN 37235, USA

<sup>b</sup> Department of Electrical Engineering, Vanderbilt University, 255 Featheringill Hall, 400 24th Ave. South, Nashville, TN 37235, USA

Received 26 September 2003; received in revised form 2 February 2004; accepted 16 April 2004

## Abstract

We introduce a synchrony map that translates the fine temporal organization of multi-unit responses in the visual cortex into an easily interpreted spatial display. We test the synchrony map on microelectrode array recordings in Area 17 of anesthetized and paralyzed cats. We first examine the synchrony map using averaged data and probability calculations to demonstrate orientation-dependent changes in synchrony. We then demonstrate how the synchrony map can be implemented for real-time visualization of synchrony among neural assemblies.

© 2004 Elsevier B.V. All rights reserved.

**Keywords:** Cortex; Synchronization; Synchrony map; Spike timing

## 1. Introduction

Synchronization is an intriguing aspect of biological systems, whether it is a flock of birds that transform into a seemingly single entity or the professional baseball player that connects with a 100-mph fastball. While the presence of synchronized nerve impulses within the brain is becoming increasingly apparent, the role played by this activity in brain function is less obvious (Salinas and Sejnowski, 2001; Usrey and Reid, 1999). One theory that has been hotly debated is that synchrony binds the individual features of an object in our visual system (Castelo-Branco et al., 2000; Eckhorn et al., 1988; Gray et al., 1989; von der Malsburg, 1981; Thiele and Stoner, 2003; see also *Neuron*, Issue 24, 1999). Coordinated timing has also been proposed as a computationally efficient form of neural processing (Hopfield, 1995; Milton and Mackey, 2000; Wyss et al., 2003). Visualizing synchrony has involved the implementation of sophisticated analytical tools and has been limited to post-experimentation (Aertsen et al., 1989; Aronov et al., 2003; Chapin and Nicolelis, 1999; Dayhoff and Gerstein, 1983; Gerstein et al., 1985; Grun et al., 2001a,b; Johnson et al., 2001; Kralik et al., 2001; Laubach et al.,

1999; Martignon et al., 2000). Because synchrony inherently depends on the form of visual stimulation and the selection of cells in multi-neuronal recordings is essentially random, some form of real-time visualization of synchrony is required to pursue its significance. We introduce a tool that translates the high-resolution (ms) organization of multi-cell activity into an easily interpreted spatial display. The display can be viewed as a static graph or a video and can be implemented either post-experimentally or preferably in real-time.

Fig. 1 shows an example of the typical feedback (Bionics NSAS Activity Map Viewer v1.0) that is used to assess neural activity using the 5 × 5 Utah Intracortical Electrode Array (UIEA) (Bionics, Salt Lake City, UT). The snapshots of the activity map represent the average firing rate over 2 s and 509 trials for three different orientation variations of a drifting sinusoid grating. Only single-unit activity for six of the 25 electrodes is shown (here 23 electrodes recorded single-unit activity) and one of the six cells fires at 5 sps or less, so it is not apparent on the activity map. During experimentation, the Bionics Activity Map feedback is provided in real time with the displayed rates calculated over an adjustable integration time (e.g., 100 ms) and an adjustable colormap range (i.e., peak and eccentricity). In addition, raster plots and event windows (similar to triggered oscilloscope displays) may also be used for real-time feedback of neural activity.

\* Corresponding author. Tel.: +1-615-322-2903; fax: +1-615-343-6702.

E-mail address: ab@vuse.vanderbilt.edu (A.B. Bonds).

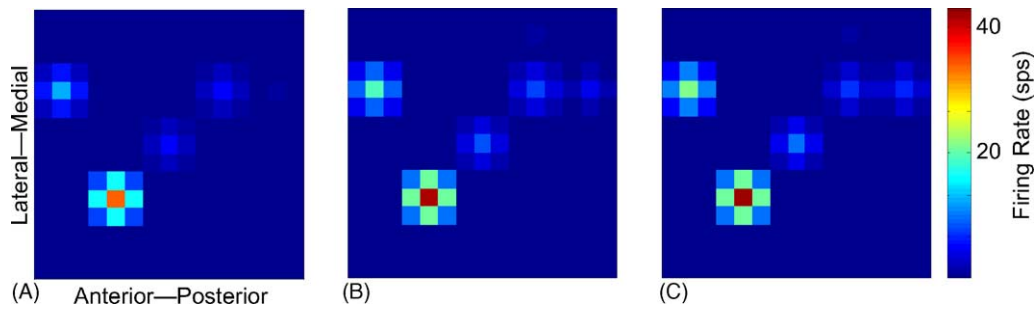


Fig. 1. An example of a display adapted from the Bionics Activity Map Viewer used in multi-electrode array recordings (see <http://www.cyberkineticsinc.com/download.htm> for details). (A) Firing rate (sps) activity map for a grating perturbed  $14^\circ$  from the preferred orientation determined for the group. (B) Activity map for a grating perturbed  $4^\circ$  from the preferred orientation. (C) Activity map for a grating at the preferred orientation.

Information from the activity map can be used to estimate the preferred orientation of a group of cells (orientation that results in the largest average firing rate). Fig. 1A ( $14^\circ$  from the preferred orientation) clearly shows less activity than Fig. 1C (at the preferred orientation), but for only a  $4^\circ$  difference in orientation (Fig. 1B vs. Fig. 1C) the distinction is less clear. The typical real-time feedback provided in multi-unit recordings (activity map, raster plot, and event monitoring) can only approximately reveal the activation from certain forms of visual stimulation. While the information available can also include the spatial organization of activity, it does not reveal anything about any temporal structure of the response or dependencies that might be occurring among the population of cells (e.g., correlated or synchronized firing).

The temporal structure of responses (de Ruyter van Steveninck et al., 1997; Richmond and Optican, 1987; Victor and Purpura, 1996) and the correlated firing between cells (Dan et al., 1998; Samonds et al., 2003, 2004a) carries stimulus-related information. The structure and correlation can be very precise (Bair, 1999; Grothe and Klump, 2000; Lestienne, 2001; Mainen and Sejnowski, 1995; Samonds and Bonds, 2004). The correlation theory predicts that the binding of cell assemblies occurs with a precision of 2–5 ms (von der Malsburg, 1981). The basic idea of the correlation theory is that features are grouped or separated through the synchrony or asynchrony of groups of cells, respectively, depending on their perceptual significance (multi-featured object, background, etc.). Support for the theory comes from evidence of changes in correlated firing that are not predicted by changes in the firing rate (Castelo-Branco et al., 2000; Eckhorn et al., 1988; Frostig et al., 1983; Gray et al., 1989; Vaadia et al., 1995). In addition to the correlation theory, studying synchrony has been essential in progressing in the understanding of neural function and pathology—e.g., schizophrenia (Green et al., 1999; Spencer et al., 2003).

Almost all of the analytical tools used to explore temporal dependencies in a population of neural recordings require large amounts of data and are limited to post-experiment calculations. The complexity of the analysis to identify tem-

poral dependencies and the statistical analysis of the reliability of the analysis severely limits any online applications of the methods. At the same time, the fundamental basis of the correlation theory is that the coordination of cells on short temporal scales inherently depends on the incoming visual information (von der Malsburg, 1981). The synchrony between cells will depend on multiple simple (Ts'o et al., 1986) and complex (Castelo-Branco et al., 2000; Eckhorn et al., 1988; Gray et al., 1989) features of visual stimuli. Because in vivo recording provides us with a relatively very small sample of the population of cells (even within the limited region covered by the electrode array) and the sample of cells is essentially “blind”, a large portion of the experimentation time is required just to determine roughly what stimulation *might* lead to correlated firing. In order to test the role of synchrony and the temporal binding hypothesis meaningfully and rigorously, real-time feedback about neural synchrony is needed. The real-time feedback will allow development of better stimulation protocol strategies to provide more detailed and consequential results.

## 2. Methods

We introduce our visualization of synchrony with post-experimentation procedures in order to provide a clearer picture for interpretation before introducing the real-time application of this tool. The visualization is founded on the sorting procedure used by Johnson et al. (2001) for making information-theoretic calculations (see also Samonds et al., 2003, 2004a). Using the temporal information (time bins) that the sorting procedure identifies, we create a *synchrony map* to identify the strength of synchrony. This map *should not be confused with the Bionics Activity Map Display in Fig. 1* despite its similar appearance. Post-experimentation use of this synchrony map provides us with an average appearance of the synchrony map displaying the temporal coordination beyond what would be expected by chance. Last, we show how the synchrony map can be utilized for its intended purpose of real-time visualization.

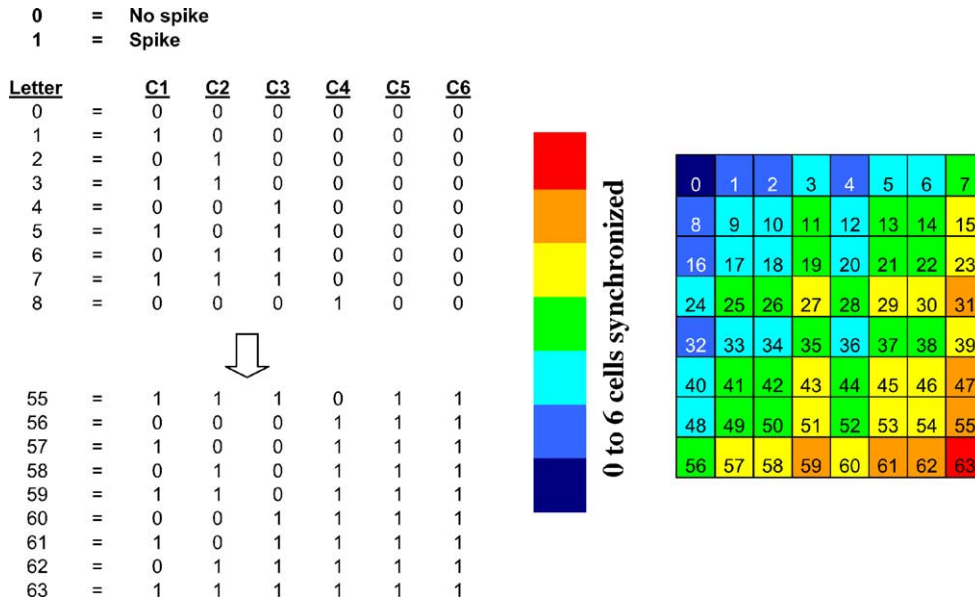


Fig. 2. Digitization procedure for converting spike patterns into letters or patterns (left). Colormap of the letters or patterns displaying how many cells are active for a particular letter.

### 2.1. Organization of synchrony map

A group of responses from a selected population of cells is broken down into discrete temporal bins and assigned a *letter* depending on which cells fired within that bin. The term letter should not be confused with the literal definition, and it is simply a term originating from communications theory (also, a set of letters is an *alphabet*). We will refer to letters as *patterns* and the alphabet as the group of possible patterns throughout the article because that is plainly what the letters represent. Fig. 2 (left) shows an example of the patterns for a six-cell population. For six cells, there are  $2^6 = 64$  possible firing patterns within a single bin (0–63). We assign the patterns as binary numbers (e.g., 101001), and then convert the binary numbers to decimal numbers (e.g., 41) for faster recognition by the program. The colormap on the right of Fig. 2 displays a color for each pattern that reflects the number of cells that fired within a single bin, according to the definition of the pattern. By simply organizing the patterns in numeric order, the synchrony map does not express much information on correlated activity that may be interpreted rapidly.

In Fig. 3, we reorganize the synchrony map so that spike activity—from zero cells firing within a bin to all six cells firing within a bin—is arranged along the diagonal from the upper left corner to the lower right corner, respectively. The patterns are also to some extent arranged from cell 1 to cell 6 along the diagonal from the lower left corner to the upper right corner, respectively (i.e., orthogonal to the number of cells firing in a pattern). The organizational principle is that the strength of the synchronization is represented diagonally from left to right and top to bottom (going from weak to strong). Asynchrony occurs when only one cell fires within

a bin, while strong synchrony occurs when *all six cells* fire within a bin.

### 2.2. Post-experimentation view of normalized synchrony

The occurrence of multi-cell firing within a bin will simply increase either with higher firing rates of the cells or larger bins. To assess whether the synchrony map actual signals differences in the synchrony rather than just

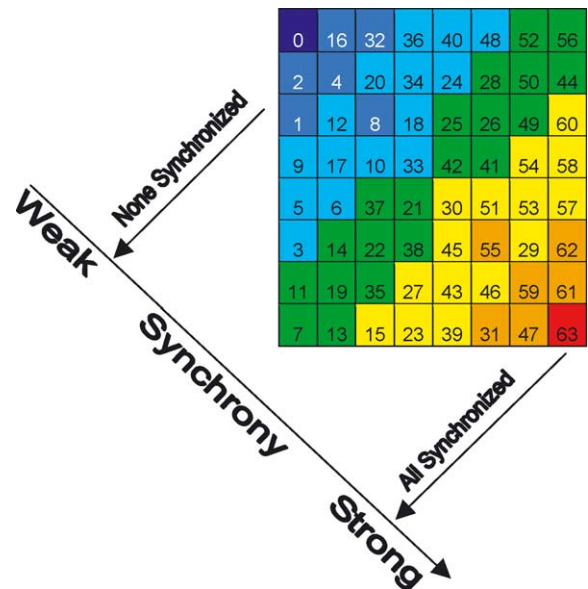


Fig. 3. A reorganized colormap from Fig. 2 to orient no synchrony in the upper left corner and strong synchrony in the lower right corner. Orthogonally, the patterns roughly incorporate cell 1 (lower left) to cell 6 (upper-right).

re-emphasizing changes in the firing rate, we establish a normalization procedure to produce a synchrony map that shows the variation of pattern occurrences from what would be expected by chance based on the cells' firing probabilities. Our intended purpose of the post-experimentation synchrony map is not to introduce a novel statistically reliable method of identifying synchronized assemblies. We are only providing a view of an *average* application of the real-time synchrony map to visualize how synchrony patterns might change with variations in visual stimulation. The first step is to calculate the empirical or observed probability  $P$  of each pattern  $k$  occurring in each bin  $b$  from  $M$  stimulus repetitions:

$$P(k, b) = \frac{\text{\#occurrences}}{M} \quad (1)$$

Next, we normalize the probability of each pattern occurring based on the probabilities of each cell firing. The normalization is essentially an ad hoc method that we derived from the quantitative measurement of neural *dependency*, which quantifies the variation of probabilities from independence based on mutual exclusivity (Johnson et al., 2001; Samonds et al., 2003, 2004a). The first step in normalization is to calculate the expected or independent probability  $P_i$  of each pattern  $k = 0$  to  $63$  occurring based on the average probability of each cell (cell one through six or c1–c6) firing within a bin. The independent probability of a pattern  $p_i$  is equal to the product of the appropriate probabilities of each cell either firing or not firing (see also Fig. 2, left):

$$P_i(1, b) = P(c1) \times (1 - P(c2)) \times (1 - P(c3)) \times (1 - P(c4)) \times (1 - P(c5)) \times (1 - P(c6))$$

$$P_i(63, b) = P(c1) \times P(c2) \times P(c3) \times P(c4) \times P(c5) \times P(c6)$$

$$(2)$$

The pixel in the synchrony map SM for each bin  $b$  is then assigned the value according to the arrangement described in Fig. 3:

$$SM(k, b) = \frac{P(k, b) - P_i(k, b)}{P_i(k, b)} \quad (3)$$

The sequence of synchrony maps (using a contour map of the SM values) from  $b = 1$  to  $B$  is then used to produce an animation of the synchrony ( $b$  can be viewed as a dimension of time).

Although we describe the normalization for Eq. (3) as an ad hoc procedure, we derived the procedure on the basis of how well the synchrony maps express differences in the synchrony of cell assemblies (for video displays). As a reference for differences in synchrony we used dependency (Samonds et al., 2004a). We did not directly use the dependency method to quantify the variation from patterns occurring simply from chance (independence) because that method was based on the quantification of the difference across *all* patterns. The difference between  $\log_2(P)$  and  $\log_2(P_i)$  (see Johnson et al., 2001 and Samonds et al., 2003, 2004a for details) distorted the map towards strong

synchrony, while the difference between  $P$  and  $P_i$  distorted the map towards asynchrony (because the synchronous patterns have such small probabilities). Eq. (3) provided the clearest distinction between asynchrony and synchrony. We must emphasize that this approach leads to a method for qualitative visualization during real-time applications (that we introduce below). The measurement of dependency, with the necessary tests of statistical significance, provides a more formal and *quantitative* assessment of the dependence among a population of cells (Samonds et al., 2003, 2004). Additionally, more formal methods are available of *identifying* synchronous events with the appropriate statistical analysis for post-experimental data analysis (e.g., Grun et al., 2001a,b).

We also calculate which pixels in the synchrony map are typically more active than chance by averaging the SM values over  $B$  bins. Because Eq. (3) can be positive or negative and an occurrence of five- to six-cell patterns will lead to such large values (because  $P_i$  is so low) we would end up with a false indication of an overbearing presence of synchrony (larger cell patterns) by simply averaging the SM values. We more accurately represent which pixels are most active across bins by normalizing for the maximum SM value for each bin:

$$SM_{\text{avg}}(k) = \frac{1}{B} \sum_{b=1}^B \frac{P(k, b) - P_i(k, b)}{P_i(k, b)} / \max_{k=0}^{63} \left[ \frac{P(k, b) - P_i(k, b)}{P_i(k, b)} \right] \quad (4)$$

### 2.3. Real-time visualization of synchrony

For real-time visualization of synchrony, we employ an 8-bit grayscale map for the synchrony map. The data are sampled at the bin width (e.g., 6–10 ms or 100–167 Hz) and each pixel is assigned a pattern according to the digitization procedure described above. A bin width of 6–10 ms is chosen based on the past analysis of the temporal resolution of the synchrony on the tested set of data (Samonds et al., 2004a,b) and can be adjusted with respect to each individual application. Because of the high sampling rate and because *only one pattern can be assigned to any single bin*, we subdivide the display into 20 bin (120–200 ms) intervals. If a particular pixel is activated at any time within that interval, the pixel is held on until completion of the interval. All pixels are then cleared and the process starts again. Holding therefore does not correspond to a sliding-window integrator or convolution. The hold duration can also be adjusted depending on experimental conditions and the ability of the experimenter to perceive highlighted pixels.

Even though the images collect pixels over 120–200 ms intervals, the image is not displayed at a slower frequency. In other words, the video display is still shown at 100–167 Hz. The high frame rate is beyond the capability of most typical monitors and is even beyond what the experimenter would

even be able to perceive. A slower display rate is not used because the temporal resolution of the synchronization demands 6 ms bin widths. Because we hold the active pixels (therefore falsely displaying a collection of active pixels) for up to 20 bins, the experimenter can still clearly identify what pixels are activated while still perceiving a very high sampling rate.

Because the patterns associated with strong synchrony (e.g., 6 cells firing simultaneously) occur so infrequently, we enhance these pixels by using increasing brightness from single-cell patterns to six-cell patterns. Black pixels (no activity) have a value of zero, while white pixels (six-cell pattern) have a value of 255 (covering the entire 8-bit range). Single-cell patterns have values of 130; two-cell patterns, 155; three-cell patterns, 180; four-cell patterns, 205; and five-cell patterns, 230. The variation in brightness provides an additional cue to enhance the identification and retention of any of the rare higher-number-of-cell-patterns (i.e., strong synchrony) being displayed.

### 3. Results

We tested the synchrony map methods on the UIEA recordings described in Samonds et al. (2004a). Figs. 4 and 5 (as well as the downloadable videos) are representative examples from one of the four synchronized six-cell assemblies described in our previous study for post-experimentation and real-time visualization of synchrony, respectively. Other examples from our recordings offer qualitatively similar impressions, indicating that the procedure is sufficient for subjective representation of degrees of synchronization. We did not apply statistical analyses to the procedure since it is solely for this purpose, and in all cases quantitative analysis was subsequently done off-line.

#### 3.1. Post-experimentation view of normalized synchrony

Fig. 4A represents a sample of 10 frames or 60 ms of multi-unit activity displayed with the post-experiment

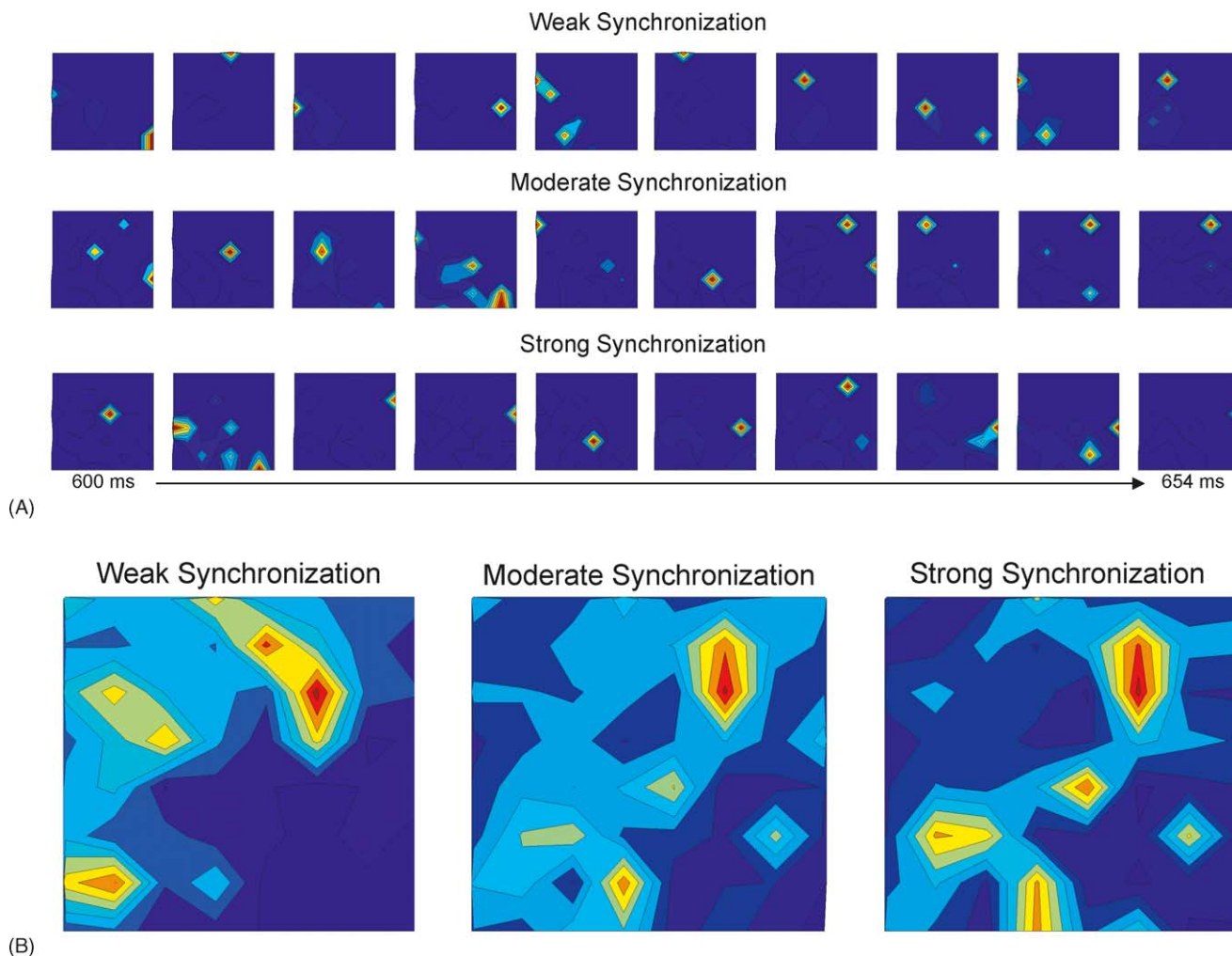


Fig. 4. Synchrony map using probability calculations of patterns (pixels) occurring normalized by the probabilities of occurrence expected simply by chance. (A) A sample of 10 frames for three levels of synchrony. The synchrony maps use contour mapping with the standard hot-cold color scale to represent large chances of occurrence (red) versus relatively small chances of occurrence (blue). (B) Average synchrony map of letters (pixels) based on which patterns occur most often (for 509 responses of 2 s each, 6 ms bins).

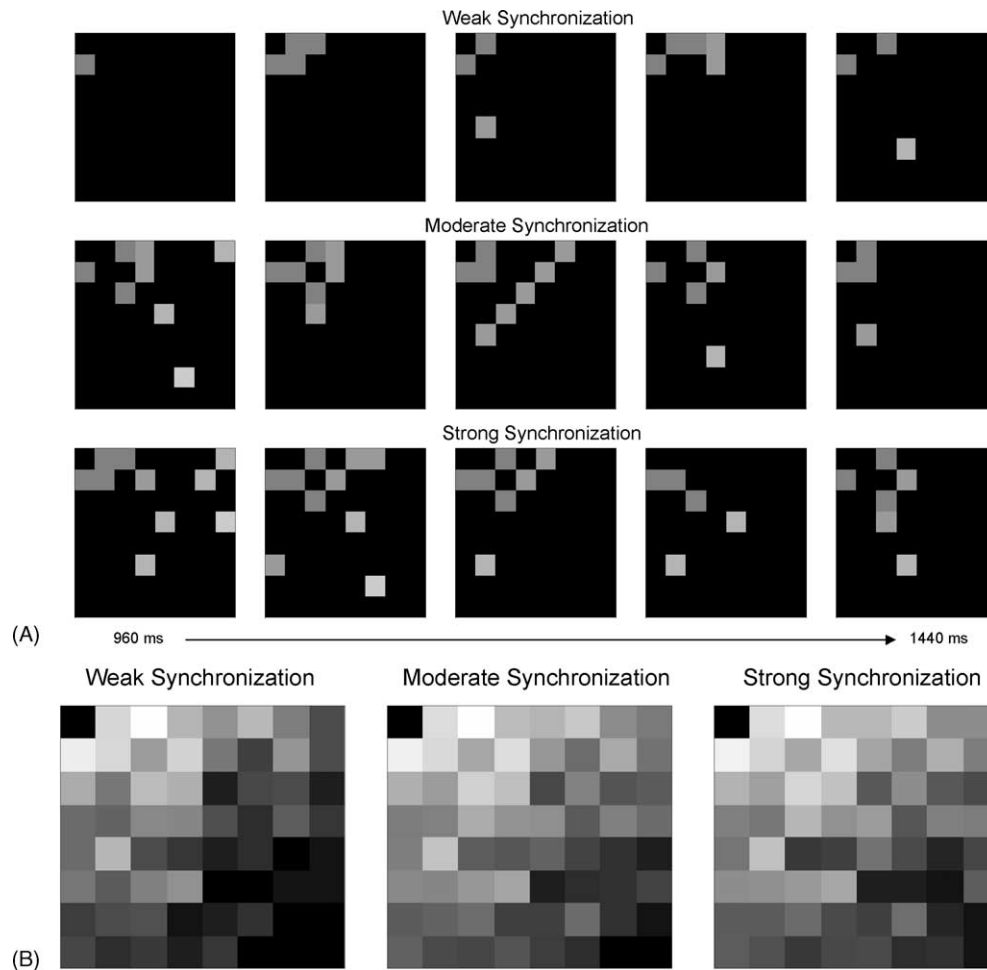


Fig. 5. An example of the real-time synchrony map. (A) A sample of accumulations of 20 frames (100 total frames, 6 ms frames) for three levels of synchrony. (B) A synchrony map of overall pattern probabilities (brighter pixels are higher probabilities) that has been enhanced for the lower probabilities.

normalized synchrony map. Windows Video Clips (.avi files) are also available on the web of the entire set of frames for each sample shown in Fig. 4A: [http://www.vuse.vanderbilt.edu/~samondjm/lab/synchrony\\_map\\_videos.htm](http://www.vuse.vanderbilt.edu/~samondjm/lab/synchrony_map_videos.htm). In the case of post-experiment viewing of the normalized synchrony map, the frame rate was reduced 10-fold (16.7 Hz) so that each 20-s video represents 2 s of average neural activity (509 trials). The reduced frame rate enables perception of the synchronous activity and accommodates the sweep speeds of most monitors. Synchrony was classed as weak, moderate and strong, with reference to quantitative dependency analysis (Samonds et al., 2003, 2004a). The weak synchrony (dependency rate, 3.6 bits/s; 47% of the dependency rate for the preferred orientation) is the activity response to a drifting sinusoid grating  $14^\circ$  from the preferred orientation of the assembly. The moderate synchrony (6.6 bits/s; 87%) is the response to  $4^\circ$  from the preferred orientation and the strong synchrony (7.6 bits/s) is the response to the preferred orientation. The three defined levels of synchrony are based on an orientation tuning function of the dependency (preferred orientation corresponds to the peak of the dependency tuning function

or the greatest amount of dependence among the six-cell assembly).

Although the differences between the three levels of synchrony are much clearer while viewing the video, Fig. 4A also reveals these differences using only 10 of the 334 computed frames for the averaged response. We use a contour map for post-experimentation viewing of the synchrony map only to provide a smoothed version of the synchrony map, since we are presenting an average representation of the data. The relationship between neighboring pixels (by cell and number of cells; see Fig. 3) makes the contour map ideal for smoothing. The contour map is normalized so a color-scale legend is inappropriate (i.e., the display shows relative differences between SM values). The response amplitude is less important than the spatial location of contours for the synchrony map. We should note that the scale is the typical hot-cold (red-blue) range (e.g., see Fig. 1) where hot represents occurrences above chance and cold represents occurrences below chance. Red is the largest SM value, while blue is the lowest SM value. We also emphasize using Fig. 3 as a guide when interpreting Figs. 4 and 5, as well as the videos. The largest SM values for weak synchrony tend to

occur in the upper left region. The largest SM values for the moderate synchrony occur in the center region with a subtle tendency towards the lower right region. The largest SM values for the strong synchrony occur even more often in the lower right region (i.e., strong synchrony). The hot spots (red) are focused and relatively random (for these 10 frames) so the difference between the three levels of synchrony can be seen more clearly by looking at the more subtle contour differences (i.e., rises), which are represented by the black lines.

In order to quantify the differences for a direct demonstration of what may clearly be seen in the videos, we create a synchrony map of the average frame seen by the observer (see Section 2.2 for details). The synchrony map averaged across all the bins or frames (see Fig. 4B) determines which patterns (or pixels) tend to have the largest SM values more often. The high points of the contour map move visibly from weak synchrony to stronger synchrony (using Fig. 3 as a guide) in the cases shown. Although the moderate synchrony and strong synchrony maps are similar, there is a clear difference in the contour map for the 4° difference in orientation. In the strong synchronization example, the contour (and therefore, relative occurrence) is lowered in the weak synchrony region and the peaks are increased in the stronger synchrony region.

When looking at the strong synchrony map, the distinction as “strong” synchrony might seem inappropriate since activation is not focused in the lower right quadrant. We have found that in groups as large as six cells (taken from populations of about 25 cells) some cells do not tend to synchronize at the preferred orientation or for any of the stimuli we tested. For all of the pairs, we tested within the six-cell assemblies, 82.3% had noticeable synchrony (Samonds et al., 2004a). While this is quite high, the probabilities of all cells synchronizing simultaneously are vanishingly low. In the particular example of Fig. 4B, the first cell (c1) included in the assembly had a relatively weak response (<5 sps) and in turn, weak synchronization with the other five cells. However, we would expect larger UIEAs (e.g., 10 × 10) to provide larger samples of cells (e.g., >50) and in turn reveal larger and stronger synchronized assemblies (J.M. Samonds, Z. Zhou, H.A. Brown, A.B. Bonds, unpublished observations). Our percentage of synchronized pairs within groups of similar orientation preference with the 5 × 5 UIEA (82.3%) is similar to the percentage of synchronized pairs based on similar orientation preference found with two electrodes (75%) (Ts’o et al., 1986), so we would predict a similar relationship with greater numbers of simultaneous recordings.

The averaged contour map in Fig. 4B also gives us some indication of which cell patterns occur more often or at least which cells fire more often. The bias towards the upper-right corner is due to the relatively higher firing rate of the sixth cell (c6) included in the assembly (see Fig. 1). There is also some enhancement in the contour map due to the second most active cell, the second cell (c2). However, the synchrony map does not provide a straightforward tool for iden-

tifying which cells tend to link through synchrony. The synchrony map is instead intended to determine the aggregate synchrony across a particular group of cells rather than to identify a synchronous subgroup within a larger group.

### 3.2. Real-time visualization of synchrony

The transition of the synchrony map to a real-time tool is not necessarily straightforward. The post-experiment synchrony maps represented changes in the occurrence of pixels relative to what would be expected by chance. The averaging and probability estimation required for these calculations cannot be definitively executed until the collection of all the data, hence there is no guarantee that the real-time synchrony map does not just re-emphasize changes in the overall activity of the cell rather than changes in the strength of synchrony. Without the probability estimations, formal statistical tests cannot be applied. However, the high temporal resolution (small bin size) results in relative small probabilities of any particular pattern and drastically smaller probabilities of the patterns indicating strong synchrony. In our example (see Fig. 1), the average probability of a cell firing within a single bin is about 1/10. Assuming independence, each five-cell pattern only has a 1/100,000 chance of occurring and the probability of all six cells firing within the same bin is 1/1,000,000. So the observation of *any* of these patterns or in fact any shift towards the strong synchrony region over the course of a few seconds would indicate that these patterns are occurring far beyond chance and that the cells are strongly synchronized. For example, even though the six-cell pattern occurs only about 10 times over 509 responses of 2 s each, this is a probability of 1/17,000, which is 60-fold greater than what we would expect simply by chance, obviating the need for formal statistical tests. The differences are even more dramatic as we focus on particular five-cell activity patterns.

Most of the activation will nonetheless tend to occur towards the weak synchrony region. This means that some interval of data collection will be required for reliable identification of different states of synchrony. Since we are examining a probabilistic system, the tool must be applied over a handful of trials (with hundreds of bins) in order to observe strong synchrony. Although this constraint seems to contradict the idea of real-time observation of synchrony, in practice strong synchrony is readily seen when present.

Fig. 5A shows a sequence of 5 sections, each with activity accumulated over 20 bins. Each picture thus represents 120 ms of accumulated activity and the sequence of 5 pictures represents the activity over a 600 ms stimulation period. All the real-time synchrony maps are samples from the same dataset used to construct the post-experiment synchrony maps shown in Fig. 4. The three examples of real-time synchrony maps demonstrate an abundance of activation in the region of asynchrony, but clearly even one 600 ms slice of activity can show greater activation towards the regions of stronger synchronization. The difference

between the three levels of synchrony is even clearer when looking at the videos that have a sample of 10 2-s trials for each orientation (see the website above).

Fig. 5B reemphasizes the fact that while most activity occurs in the asynchronous region of the synchrony map, there are clear differences between the three levels of synchrony. The three images represent the total probability (across all trials and all bins) of each pattern occurring, where white represents the highest probability and black represents a probability of zero. In order to show the differences between each level of synchrony, we enhanced the pixels in the strong synchrony region of the map by taking the log of each probability. The procedure enhances the patterns or pixels in the lower right corner so that differences are clearer in that region.

#### 4. Discussion

We have introduced a straightforward method that permits rapid identification of the strength of synchrony of a small group of simultaneously recorded cells. The most important aspect of this method is that we translate detailed temporal information (i.e., synchrony) into easily identifiable spatial information with the synchrony map. We tested the synchrony map on microelectrode array recordings (Samonds et al., 2004a) by first using probabilities calculated from the repetitions of recordings and normalized for the synchrony that would occur simply from chance. With the real-time synchrony map, we demonstrated that despite the rarity of very strong synchronization (even when it occurs far beyond chance), subtle differences in synchrony can be identified with the synchrony map because of the temporal-to-spatial translation of information. The synchrony map enhances experimental planning by helping to isolate stimuli that result in synchronization. Once those circumstances are roughly identified, an efficient stimulus protocol can be combined with offline analysis for formal identification and quantification of neural cooperation.

##### 4.1. Details about cooperation

We have tested the synchrony map on data that we analyzed for cooperative discrimination of orientation (Samonds et al., 2004a). The analytical methods (type analysis; see Johnson et al., 2001) we employed in the study were virtually unconstrained, making it difficult to draw any definitive conclusions about the nature of the neural coding. We were able to show that synchronous activity likely contributed to cooperative discrimination of fine angle differences by looking at the dependency among cells and using additional analytical methods (Aertsen et al., 1989; Gerstein et al., 1985; Samonds and Bonds, 2004). We were also able to resolve how the temporal coordination of responses can encode a small angle difference whereas the spike rate provides almost no reliable information (Samonds and Bonds, 2004).

The synchrony map (Figs. 4 and 5) compared to Fig. 1 basically confirms this notion.

In addition, the synchrony map (both post-experimentation and real-time) provides us with more detailed information than that from the nearly unconstrained methods (Samonds et al., 2004a). Type analysis produces a “distance” measurement that tells us how different two neural responses are based on classification theory. Although the distance results from the firing patterns described in this article, it does not reveal how the patterns contribute to the distance. A major technical hurdle of employing type analysis is the sampling requirements. The total number of possible response patterns exponentially grows with both population size and temporal dependencies, making it increasingly difficult to record a sufficient number of samples for adequate estimations. This underscores the importance of a synchrony map to plan experimentation, so that we can concentrate on the stimuli that yield the most meaningful response patterns.

If we had employed the synchrony map during recording we would have likely had an easier time obtaining an even better sample of synchronized cells. We focused on groups of 5–7 cells and chose groups with similar preferred orientations, which typically is a very strong indicator of synchrony (Gray et al., 1989; Samonds et al., 2004a; Ts'o et al., 1986). With the synchrony map, we would have been able to use synchrony directly as a tool for identifying groups of cells. In addition, the synchrony map would have made determining an accurate preferred orientation for the aggregate assembly much easier and in turn, resulting in a more comprehensive and meaningful range of stimulation. We will describe what we believe will be even more useful applications of the synchrony map below.

##### 4.2. Adaptation and enhancement

One of the pitfalls of the synchrony map is that the experimenter is still required to choose a candidate subgroup of cells for synchronization study. To overcome this uncertainty, the synchrony map could be examined while varying the selection of cells to be included in the pattern assignments. In addition, the choice of cells can be limited simply by observing cell activity (e.g., Fig. 1), since a synchronized group of cells will of course have to also be an active group of cells. The synchrony map is also certainly adaptable to accommodate differing numbers of cells that could be tested for synchronization. The steps described in Figs. 2 and 3 provide a straightforward method regardless of the assembly size. The size of the synchrony map merely changes with the number of cells:  $2^{\text{number of cells}}$ .

An enhancement that could be added to the synchrony map is audio feedback. Audio feedback has always been useful in neurophysiology experiments as an additional cue to real-time oscilloscope displays of single-cell electrode recordings. The action potentials result in a distinct sound in the audio output of the electrode signal so that the experimenter can estimate changes in the firing rate of the cell.

Audio feedback can enhance the synchrony map by playing sounds assigned to each bin with varying frequencies, such that activation of more cells in a pattern yields a higher frequency, similar to the variation in brightness (grayscale value) used in Fig. 5.

#### 4.3. Possible applications

Although we point out the advantages that we would have gained in applying the synchrony map to previous experiments, our purpose in developing the tool was for answering questions related to correlation theory (von der Malsburg, 1981). The main idea is that groups of cells dynamically link (through correlated or synchronized firing) depending on the features of the visual input such as object relation, context, coherence, etc. For example, one of the earliest tests of this theory was measuring changes in the synchrony between pairs of cells with the coherence of visual stimulation (light bar) of both cells (Eckhorn et al., 1988; Gray et al., 1989). From the perspective of grating stimulation, there are two examples of perceptual phenomena that can be utilized to test the correlation theory: (i) figure-ground separation (Marr, 1976) and (ii) the coherency/transparency phenomenon (Adelson and Movshon, 1982).

We are quickly able to identify multiple and overlapping objects with spatiotemporal features and organization within a background that may also have spatiotemporal features and organization. The ability to distinguish the object from the background even when both would result in similar general response characteristics when shown independently is known as figure-ground separation (Marr, 1976). The correlation theory has been one way to account for this phenomenon, but this has not received support from recordings of pairs of cells (Lamme and Spekreijse, 1998). Figure-ground separation can be tested using a circular aperture grating combined with a surrounding annular grating (Sillito and Jones, 1996). Using this stimulation protocol with microelectrode array recordings and the synchrony map (along with the traditional array feedback) will allow the experimenter to adjust the characteristics and positioning of the “figure” and “ground” grating. The relatively fast adjustment will best test the relationship of figure and ground with respect to the synchrony of various neural assemblies before collecting the large amounts of data needed for more comprehensive correlation and synchrony analysis.

When two gratings are superimposed, the gratings are either seen as a plaid moving in a single direction (coherence) or as two independently drifting gratings (transparency) depending on the relative contrasts, spatial frequencies, and directions of motion of the gratings (Adelson and Movshon, 1982). Contradictory results have been found when experimentally testing the correlation theory for the transition between coherency and transparency with pairs of cells (Castelo-Branco et al., 2000; Thiele and Stoner, 2003). Using two independent gratings, synchronized assemblies that have an ideal relationship of their respective preferred

orientations (i.e., the difference is near the coherency and transparency transition) could be identified during an experiment. Once the ideal population of cells and ideal grating characteristics are chosen, superimposed gratings can be used for meticulous testing of the correlation theory.

The examples described above are just two scenarios where the synchrony map can be utilized for real-time feedback for multi-unit recordings. As neurophysiology continues to move from the single-cell recordings to larger multi-unit recordings, tools such as the synchrony map need to be developed in order to overcome the technical and conceptual complexities that arise when studying the dynamic and multifaceted coordination that occurs among neural networks within the brain.

#### Acknowledgements

We thank John Allison and Heather Brown for their contributions in collecting the data tested with the methods described in this article. Supported by National Eye Institute Grant RO1EY-03778-20.

#### References

- Adelson EH, Movshon JA. Phenomenal coherence of moving visual patterns. *Nature* 1982;300:523–5.
- Aertsen AMHJ, Gerstein GL, Habib MK, Palm G. Dynamics of neuronal firing correlation: modulation of “Effective Connectivity”. *J Neurophysiol* 1989;61:900–17.
- Aronov D, Reich DS, Mechler F, Victor JD. Neural coding of spatial phase in V1 of the macaque monkey. *J Neurophysiol* 2003;89:3304–27.
- Bair W. Spike timing in the mammalian visual system. *Curr Opin Neurobiol* 1999;9:447–53.
- Castelo-Branco M, Goebel R, Neuenschwander S, Singer W. Neural synchrony correlates with surface segregation rules. *Nature* 2000;405:685–9.
- Chapin JK, Nicolelis MAL. Principal component analysis of neuronal ensemble activity reveals multidimensional somatosensory representations. *J Neurosci Methods* 1999;94:121–40.
- Dan Y, Alonso J-M, Usrey WM, Reid RC. Coding of visual information by precisely correlated spikes in the lateral geniculate nucleus. *Nat Neurosci* 1998;1:501–7.
- Dayhoff JE, Gerstein GL. Favored patterns in spike trains. Part I. Detection. *J Neurophysiol* 1983;49:1334–48.
- de Ruyter van Steveninck RR, Lewen GD, Strong SP, Koberle R, Bialek W. Reproducibility and variability in neural spike trains. *Science* 1997;275:1805–8.
- Eckhorn R, Bauer R, Jordan W, Brosch M, Kruse W, Munk M, Reitboeck HJ. Coherent oscillations: a mechanism of feature linking in the visual cortex? *Biol Cybern* 1988;60:121–30.
- Frostig RD, Gottlieb Y, Vaadia E, Abeles M. The effects of stimuli on the activity and functional connectivity of local neuronal groups in the cat auditory cortex. *Brain Res* 1983;272:211–21.
- Gerstein GL, Perkel DH, Dayhoff JE. Cooperative firing activity in simultaneously recorded populations of neurons: detection and measurement. *J Neurosci* 1985;5:881–9.
- Gray CM, Koehnig P, Engel AK, Singer W. Oscillatory responses in cat visual cortex exhibit inter-columnar synchronization which reflects global stimulus properties. *Nature* 1989;338:334–7.

- Green MF, Nuechterlein KH, Breitmeyer B, Mintz J. Backward masking in unmedicated schizophrenic patients in psychotic remission: Possible reflection of aberrant cortical oscillation. *Am J Psychiatry* 1999;156:1367–73.
- Grothe B, Klump GM. Temporal processing in sensory systems. *Curr Opin Neurobiol* 2000;10:467–73.
- Grun S, Diesmann M, Aertsen A. Unitary events in multiple single-neuron spiking activity: Part I. detection and significance. *Neural Comp* 2001a;14:43–80.
- Grun S, Diesmann M, Aertsen A. Unitary events in multiple single-neuron spiking activity: Part II. Nonstationary data. *Neural Comp* 2001b;14:81–119.
- Hopfield JJ. Pattern recognition computation using action potential timing for stimulus representation. *Nature* 1995;376:33–6.
- Johnson DH, Gruner CM, Baggerly K, Seshagiri C. Information-theoretic analysis of neural coding. *J Comp Neurosci* 2001;10:47–69.
- Kralik JD, Dimitrov DF, Krupa DJ, Katz DB, Cohen D, Nicolelis MAL. Techniques for long-term multisite neuronal ensemble recordings in behaving animals. *Methods* 2001;25:121–50.
- Lamme VAF, Spekreijse H. Neural synchrony does not represent texture segregation. *Nature* 1998;396:362–6.
- Laubach M, Shuler M, Nicolelis MAL. Independent component analysis for quantifying neuronal ensemble interactions. *J Neurosci Methods* 1999;94:141–54.
- Lestienne R. Spike timing, synchronization and information processing on the sensory side of the central nervous system. *Prog Neurobiol* 2001;65:545–91.
- Mainen ZF, Sejnowski TJ. Reliability of spike timing in neocortical neurons. *Science* 1995;268:1503–6.
- Marr D. Early processing of visual information. *Philos Trans R Soc Lond B Biol Sci* 1976;275:483–519.
- Martignon L, Deco G, Laskey K, Diamond M, Freiwald W, Vaadia E. Neural coding: higher-order temporal patterns in the neurostatistics of cell assemblies. *Neural Comp* 2000;12:2621–53.
- Milton JG, Mackey MC. Neural ensemble coding and statistical periodicity: Speculations on the operation of the mind's eye. *J Physiol* 2000;94:489–503.
- Richmond BJ, Optican LM. Temporal encoding of two-dimensional patterns by single units in primate inferior temporal cortex. Part II. Quantification of response waveform. *J Neurophysiol* 1987;57:147–61.
- Salinas E, Sejnowski TJ. Correlated neuronal activity and the flow of neural information. *Nat Neurosci Rev* 2001;2:539–50.
- Samonds JM, Bonds AB. From another angle: differences in cortical coding between fine and gross discrimination of orientation. *J Neurophysiol* 2004;91:1193–202.
- Samonds JM, Allison JD, Brown HA, Bonds AB. Cooperation between area 17 neuron pairs enhances orientation discrimination. *J Neurosci* 2003;23:2416–25.
- Samonds JM, Allison JD, Brown HA, Bonds AB. Cooperative synchronized assemblies enhance orientation discrimination. *Proc Natl Acad Sci USA* 2004a;101:6722–7.
- Samonds JM, Brown HA, Bonds AB. Relationships between the spatiotemporal spike train structure and cortical synchronization. *J Vision* 2004b; abstract, in press.
- Sillito AM, Jones HE. Context-dependent interactions and visual processing in V1. *J Physiol (Paris)* 1996;90:205–9.
- Spencer KM, Nestor PG, Niznikiewicz MA, Salisbury DF, Shenton ME, McCarley RW. Abnormal neural synchrony in schizophrenia. *J Neurosci* 2003;23:7407–11.
- Thiele A, Stoner G. Neural synchrony does not correlate with motion coherence in cortical area MT. *Nature* 2003;421:366–70.
- Ts'o DY, Gilbert CD, Wiesel TN. Relationships between horizontal interactions and functional architecture in cat striate cortex as revealed by cross-correlation analysis. *J Neurosci* 1986;6:1160–70.
- Usrey WM, Reid RC. Synchronous activity in the visual system. *Annu Rev Physiol* 1999;61:435–56.
- Vaadia E, Haalman I, Abeles M, Bergman H, Prut Y, Slovin H, Aertsen A. Dynamics of neuronal interactions in monkey cortex in relation to behavioural events. *Nature* 1995;373:515–8.
- Victor JD, Purpura KP. Nature and precision of temporal coding in visual cortex: a metric-space analysis. *J Neurophysiol* 1996;76:1310–26.
- von der Malsburg C. The correlation theory of brain function. Göttingen, Germany: Max-Planck Institute for Biophysical Chemistry internal report; 1981.
- Wyss R, König P, Verschure PF. Invariant representations of visual patterns in a temporal population code. *Proc Natl Acad Sci USA* 2003;100:324–9.